Eur. J. Mineral.
1997, **9**, 935-940

Raman spectra of various types of tourmaline

BILIANA GASHAROVA*, BORIANA MIHAILOVA** and LUDMIL KONSTANTINOV**

*Forschungszentrum Karlsruhe GmbH, ITC-WGT, Department of Technical Mineralogy,
P.O. Box 3640, D-76021 Karlsruhe, Germany
e-mail: biliana.gasharova@itc-wgt.fzk.de
**Central Laboratory of Mineralogy and Crystallography, Bulgarian Academy of Sciences,
Rakovski St. 92, 1000-Sofia, Bulgaria
e-mail: mincryst@bgcict.acad.bg

Abstract: A large number of different tourmalines are investigated by Raman spectroscopy in the spectral range 150–1550 cm^{-1}. According to their chemical composition, the studied tourmalines can be classified into three main groups: buergerite-schorl, G1; elbaite-type, G2; and dravite-buergerite-uvite, G3. It is shown that the same classification of tourmalines can be established on the basis of their Raman spectra. Bands for G1 are centred at about 230 and 670 cm^{-1}, the spectra being characterized by a single peak at 238 ± 2 cm^{-1} and three resolved peaks at 635 ± 3, 674 ± 3 and 697 ± 3 cm^{-1}; G2 has a sharp peak at 224 ± 2 and two well separated peaks, one at 638 ± 3 cm^{-1} and the other higher than 707 cm^{-1}; G3 is characterized by two peaks at 215 ± 3 and 237 ± 3 cm^{-1}, with a smoothed spectral band centred at about 670 cm^{-1}.

Key-words: tourmaline, Raman spectroscopy.

Introduction

Tourmalines have recently attracted much interest due to the significant variations observed in their composition within one and the same type of structure. The tourmaline group of minerals has been most generally described by the formula $XY_3Z_6(BO_3)_3[(Si,Al)_6O_{18}](O,OH)_3(OH,F)$, where X = Na,Ca,Mg,□; Y = Li,Mg,$Fe^{2+/3+}$,Al, Ti,□ and Z = Mg,Fe^{3+},Al, *etc.*

Due to the large amount of substitutions in octahedral sites Y and Z, tourmalines have been usually considered in terms of the end-member components:
schorl $NaFe_3Al_6(BO_3)_3Si_6O_{18}(OH,F)_4$;
elbaite $Na(Li,Al)_3Al_6(BO_3)_3Si_6O_{18}(OH,F)_4$;
buergerite $NaFe^{3+}_3Al_6(BO_3)_3Si_6O_{18}(F,O_3)$;
dravite $NaMg_3Al_6(BO_3)_3Si_6O_{18}(OH,F)_4$;
uvite $CaMg_3(Al_5Mg)(BO_3)_3Si_6O_{18}(OH,F)_4$.

Although Raman spectroscopy has proved to be a powerful method for studying structural properties of minerals (especially the role of short- and intermediate-range ordering), it has been only sporadically applied to tourmalines. The reason is the complicated structure of these minerals, which requires sophisticated identification of the spectral peaks. So far, only the study of Griffith (1969) has systematized Raman shifts in tourmalines in terms of the vibrational modes of rings of SiO_4 tetrahedra. Alvarez & Coy-Yll (1978) have presented Raman spectra of four single crystals of tourmaline in the frequency range 100–1200 cm^{-1}, suggesting that the Si_6O_{18} rings can hardly be considered as separate vibrational units. On the contrary, a relatively recent study by Peng *et al.* (1989) reported polarized Raman spectra of tourmalines from three geological occurrences in China, in which the major peaks in the spectral range below 1200 cm^{-1} were related to modes of hexagonal $[Si_6O_{18}]^{12-}$ rings.

The present study presents the results of a detailed study of tourmalines by Raman spectroscopy in the frequency range 150–1550 cm^{-1}, where cation-oxygen vibrational modes are Ra-

0935-1221/97/0009-0935 $ 1.50

Table 1. Crystallochemical formulae of the tourmaline samples in groups G1, G2 and G3.

Sample	Crystallochemical formula
G1L	$Na_{1.00}(Mg_{0.11}Mn_{0.12}Fe^{2+}_{0.59}Fe^{3+}_{1.02}Al_{1.16})$ $Al_{6.00}B_{2.85}(Si_{5.93}Al_{0.07})O_{28.66}(OH)_{2.34}$
G1M	$(Na_{0.86}K_{0.10}Ca_{0.04})(Mg_{0.49}Mn_{0.02}Fe^{2+}_{0.26}Fe^{3+}_{1.60}Ti_{0.04}\square_{0.59})$ $Al_{6.00}B_{3.00}(Si_{5.85}Al_{0.15})O_{28.48}(OH)_{1.43}$
G1Y	$(Na_{0.78}K_{0.02}\square_{0.20})(Mg_{0.56}Fe^{2+}_{0.62}Fe^{3+}_{1.39}Al_{0.33}Ti_{0.06}\square_{0.04})$ $Al_{6.00}B_{3.00}Si_{6.00}O_{28.76}(OH)_{2.02}F_{0.02}$
G2Q	$(Na_{0.90}K_{0.02}Ca_{0.08})(Li_{0.87}Mg_{0.23}Mn_{0.16}Fe^{2+}_{0.05}Fe^{3+}_{0.10}Al_{1.59})$ $Al_{6.00}B_{3.00}Si_{6.00}O_{28.22}(OH)_{2.38}F_{0.08}$
G2C	$(Na_{0.86}K_{0.09}Ca_{0.05})(Li_{0.99}Mg_{0.27}Mn_{0.23}Fe^{2+}_{0.10}Al_{1.41})$ $Al_{6.00}B_{2.93}Si_{6.00}O_{27.26}(OH)_{3.64}F_{0.10}$
G2Z	$(Na_{0.98}K_{0.02})(Li_{0.80}Mg_{0.28}Mn_{0.34}Fe^{2+}_{0.20}Fe^{3+}_{0.38}Al_{1.00})$ $Al_{6.00}B_{3.00}(Si_{5.82}Al_{0.18})O_{27.54}(OH)_{3.32}$
G3G	$(Na_{0.60}K_{0.10}Ca_{0.30})(Mg_{2.10}Fe^{2+}_{0.25}Fe^{3+}_{0.52}Ti_{0.13})$ $(Mg_{0.08}Al_{5.92})B_{2.84}Si_{6.00}O_{28.21}(OH)_{2.10}$
G3V	$(Na_{0.21}Ca_{0.44}Mg_{0.05}\square_{0.30})(Mg_{1.39}Fe^{2+}_{0.50}Fe^{3+}_{0.91}Ti_{0.20})$ $(Mg_{0.36}Fe^{3+}_{0.91}Al_{4.73})B_{3.00}(Si_{5.92}Ti_{0.08})O_{28.47}(OH)_{2.20}$
G3T	$(Na_{0.64}K_{0.06}Ca_{0.01}\square_{0.29})(Mg_{1.72}Fe^{2+}_{0.12}Fe^{3+}_{0.60}Al_{0.56})$ $Al_{6.00}B_{3.00}Si_{6.00}O_{28.60}(OH)_{1.68}$

man-active. The aim of the study is to propose criteria for classifying these minerals on the basis of Raman spectroscopy data. For this purpose, Raman spectra of various types of tourmaline samples studied in the same experimental geometry and, on the other hand, the set of polarized Raman spectra of one of the samples are presented in order to interpret them in terms of the normal vibrational modes of clusters forming the tourmaline structure.

Experimental

Analytical techniques

The chemical composition of the samples were determined by wet chemical analysis for most elements, but by means of atom absorption spectroscopy for Li, flame photometry for Na and K, thermal analysis for OH content and, electron microprobe analysis for zoned crystals (scanning electron microscope Philips 515 SEM equipped with an EDS system). The unit cell parameters of the samples were measured using a powder X-ray diffractometer (DRON-20) with filtered cobalt radiation operating at an angular velocity of 1 deg.min^{-1} in the angular range from 7 to 30°.

Table 2. Unit cell parameters of the tourmaline samples in groups G1, G2 and G3.

Samples	a_0 (Å)	c_0 (Å)	Volume (Å^3)
G1L	16.017	7.150	1588.543
G1M	15.913	7.153	1570.640
G1Y	15.842	7.327	1592.490
G2Q	15.794	7.133	1540.944
G2C	15.837	7.101	1542.396
G2Z	15.903	7.115	1558.345
G3G	15.922	7.189	1578.317
G3V	16.031	7.242	1611.797
G3T	15.967	7.202	1590.121

Raman spectroscopy

The experiments were performed at room temperature by a Raman microspectrometer Microdil-28 (Dilor Co.) with intensified diode-array detector in back-scattering geometry at 488.0 and 514.5 nm. The Ar^+ laser beam was focused to a spot of about 1 μm diameter by a small numerical aperture microscope objective, thus making it possible to study different homogeneous parts of the samples without any inclusions or cracks. The

Raman frequencies were carefully calibrated to 1 cm^{-1} using standard Ne emission lines. Integration time constants in the range 10–50 s were used to eliminate the experimental fluctuations.

Samples

Twenty-five natural tourmaline samples from various occurrencies all over the world were investigated in this work. According to their Raman spectra, they were classified into three clear categories (see below), in which the spectra vary only slightly from one another. According to their chemical composition, these categories can be defined as follows: G1 – intermediate between buergerite and schorl, G2 – close to elbaite, and G3 – belonging to the solid solution series dravite-buergerite-uvite. Tables 1 and 2 list the crystallochemical formulae and the unit cell parameters for three representative samples of each category. The main characteristics of these samples are as follows:

G1L – a long-prismatic crystal, black in colour, found in the quartz-microcline zone of a pegmatite vein intruded into high-grade orthogneisses at Latinka, Central Rhodopes, Bulgaria,

G1M – a short-prismatic black crystal from granite pegmatite at Markova Trapeza, Plana pluton, W Bulgaria,

G1Y – a short-prismatic and brownish-black crystal of metasomatic origin from Omsukchan, Yakutia, NE Siberia,

G2Q – a long-prismatic green transparent crystal from Quebec, Canada,

G2C – a single placer crystal, dark-blue in colour and transparent, from granite pegmatites in the Southern California batholith,

G2Z – a short-prismatic, indigo-blue and transparent crystal from a rare-metal granite pegmatite, Mudzi-Rushinga, NE Zimbabwe,

G3G – a short-prismatic black crystal from a pegmatite vein intruded into leucogneisses, Oasis Schirmacher, Queen Maud Land, E Antarctica,

G3V – a short-prismatic black crystal from pegmatite veins in a calc-alkaline pluton, Vitosha mountain, Bulgaria,

G3T – a short-prismatic black crystal found in a lens-like quartz-tourmaline body intruded into mica schists, Topolovgrad, SE Bulgaria.

The spectra were recorded on well-developed natural (11$\bar{2}$0) and (10$\bar{1}$0) prism faces and on polished (0001) surfaces.

Results and discussion

Symmetry arguments

The rhombohedral structure of tourmaline has *R*3*m* symmetry (*Z* = 3) (Buerger *et al.*, 1962) and consists of linked SiO_4 tetrahedra sharing two oxygen atoms to form hexagonal Si_6O_{18} rings. In the centre of each ring, and *X*-cation is positioned which is slightly offset from the plane of the ring along the c-axis. In addition, two types of cation-oxygen octahedra are present in the structure forming various clusters, three of which, of a larger size, contain *Y*-cations, while the other six, with *Z*-cations and being smaller in size, are linked in pairs by apices. These octahedra form spiral chains along the 3_1 screw axes. On the other hand, the two types of octahedra are edge-linked in such a way that each ring of tetrahedra shares the apical oxygen atoms. Boron ions are surrounded by three oxygen atoms forming planar triangular clusters. The *Y*-centred octahedra contain two hydroxyl groups at their opposite corners. In addition, the presence of numerous substitutional atoms and vacancies complicates the tourmaline structure (Foit, 1989; Foit & Rosenberg, 1977; Hawthorne *et al.*, 1993; *etc.*).

The factor group analysis of tourmalines predicts 28 A_1 and 49 *E* Raman active modes, but it is impossible experimentally to detect all of them. The character table of the tourmaline point group determines the kind of phonons (transverse (*T*) or longitudinal (*L*)) expected in the different geometries. The corresponding polarizability tensor elements contributing to the Raman spectra are given in Table 3. In this table and in the following, we

Table 3. Modes of vibrations of the 3m(C_{3v}) point group in back-scattering geometry.

	$A_1(T)$	$A_1(L)$	$E(T)$	$E(L)$
$x(yy)\bar{x}$	α^z_{yy}			α^x_{yy}
$x(zz)\bar{x}$	α^z_{zz}			
$x(zy)\bar{x}$			α^y_{yz}	
$y(xx)\bar{y}$	α^z_{xx}		α^x_{xx}	
$y(zz)\bar{y}$	α^z_{zz}			
$y(zx)\bar{y}$			α^x_{xz}	
$z(xx)\bar{z}$		α^z_{xx}	α^x_{xx}	
$z(yy)\bar{z}$		α^z_{yy}	α^x_{yy}	
$z(xy)\bar{z}$			α^y_{xy}	

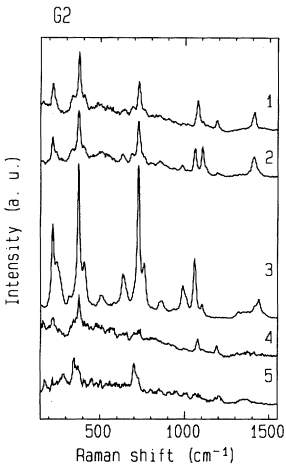

Fig. 1. Experimental Raman spectra of tourmaline G2C in various geometries: $z(xx)\bar{z}$ (curve 1), $x(yy)\bar{x}$ (curve 2), $x(zz)\bar{x}$ (curve 3), $z(xy)\bar{z}$ (curve 4) and $x(zy)\bar{x}$ (curve 5).

make use of the conventional "Porto's notation". It can be seen in Table 3 that the polarizability tensor elements are equal for the scattering geometries $z(xx)\bar{z}$ and $z(yy)\bar{z}$, $x(zy)\bar{x}$ and $y(zx)\bar{y}$ as well as $x(zz)\bar{x}$ and $y(zz)\bar{y}$ since $\alpha_{xx} = \alpha_{yy}$ and $\alpha_{xz} = \alpha_{yz}$. According to Table 3, the spectra in $x(yy)\bar{x}$ and $y(xx)\bar{y}$ geometries should differ only in the type of generating E modes. As a result, we consider only five polarized Raman spectra.

Mode assignment

Fig. 1 presents the polarized Raman spectra of sample G2C in the frequency range 150–1550 cm^{-1}, while Table 4 shows the positions of the observed peaks and the type of generating modes. The type of vibrations is determined on the basis

Table 4. Positions of observed peaks in the range 150–1550 cm^{-1} obtained by experimental Raman spectra of the sample G2C, with types of vibrational mode.

Peak label	$z(xx)\bar{z}$		$x(yy)\bar{x}$		$x(zz)\bar{x}$	$z(xy)\bar{z}$	$x(zy)\bar{x}$	Type of modes*
	$A_1(L)$	$E(T)$	$A_1(T)$	$E(T)$	$A_1(T)$	$E(T)$	$E(T)$	
P1					1442			B-O str
P2	1412		1412		1412			B-O str
P3	1190					1190		Si-O_{br} str **
P4			1105		1105			Si-O_{br} str
P5	1077					1077		Si-O_{br} str
P6			1059		1059			Si-O_{non} str
P7			989		989			Si-O str
P8					860			B-O-Al bend
P9			850					B-O-Al bend
P10	760		760		760			Si-O str & Si-O-Si bend
P11	731					731		B-O str & O-B-O bend
P12			717		717		717	"breathing" of O_{br} in Si-O rings
P13							700	B-O str & B-O-Al bend
P14	693							B-O str & B-O-Al bend
P15	641							Si-O_{br} rck
P16					637			Si-O_{br} rck
P17			632					Si-O_{br} rck
P18			508		508			oxygen vibrations in Si-O rings
P19	407		407		407			O_{non}-Si-O_{non} bend
P20	373		373		373	373	373	Al-O str
P21							350	Si-O_{non} rck
P22		340		340				Si-O_{non} rck
P23							286	O-Al-O bend
P24			244		244			O-Al-O bend
P25	222		222		222			Mg-O str, Fe-O str

* str, bond stretching; bend, bond bending; rck, bond rocking.

** O_{br}, bridging oxygens in the Si-O rings, which link two SiO_4 tetrahedra; O_{non}, non-bridging oxygens in the Si-O rings.

Table 5. Experimental frequencies (in cm^{-1}) of the observed peaks in the Raman spectra of the three representative samples (peaks are labelled as in Table 4).

Peak label	G1L	G2C	G3V	Type of modes*
P4	1056	1105	1050	Si-O_{br} str **
P6	1020	1059	1024	Si-O_{non} str
P7	969	989	973	Si-O str
P10	777	760	753	Si-O str & Si-O-Si bend
P11	780	731	765	B-O str & O-B-O bend
P12	701	727	699	"breathing" of O_{br} in Si-O rings
P14	765	693	741	B-O str & B-O-Al bend
P16	674,637	637	661,640	Si-O_{br} rck
P18	437	508	481	oxygen vibrations in Si-O rings
P19	403	407	409	O_{non}-Si-O_{non} bend
P20	369	373	365	Al-O str
P21	349	350	356	Si-O_{non} rck
P24	ov	244	ov	O-Al-O bend
P25	237	222	238,215	Mg-O str, Fe-O str

* str, bond stretching; bend, bond bending; rck, bond rocking; ov, overlaped.
** O_{br}, bridging oxygens in the Si-O rings, which link two SiO_4 tetrahedra; O_{non}, non-bridging oxygens in the Si-O rings.

of calculated spectra of small clusters with imposed boundary conditions (Mihailova *et al.*, 1994, 1996). According to our calculations, the Si_6O_{18} ring can be considered as a separate unit whose internal vibrational modes are sensitive to the neighbouring cations of the ring, *i.e.* to the type of *X*-, *Y*- and *Z*-positioned cations. On the other hand, boron-oxygen and aluminium-oxygen vibrations should be treated as modes of a combined B-Al-O network and, as a result, the modes which include symmetric B-O stretching give rise to peaks at about 750 cm^{-1}.

Due to the different optical parameters of the tourmalines in the studied groups, their Raman spectra differ substantially in intensity from each other. The best quality polarized Raman spectra in all geometries are obtained for tourmalines of group G2 (elbaite type), and only in this case it is possible to detect low-intensity peaks at about 1400 cm^{-1} arising from anti-symmetric B-O stretching vibrations. On the contrary, because the diagonal elements of the polarizability tensor are much larger than the non-diagonal elements, the measured parallel-polarized spectra are at least one order of magnitude more intense than the corresponding cross-polarized spectra. Our experimental results indicate that, for all samples, the most intense Raman spectra are those determined by the α_{zz}^{z} component of the polarizability tensor. Thus, such spectra are most suitable for obtaining structural information on tourmalines and can be recorded on $(10\bar{1}0)$ or $(11\bar{2}0)$ prism faces with laser beam polarization parallel to the c-axis of the crystal. Fig. 2 shows the spectra of samples from the three groups recorded using such an experimental scattering geometry (on $(10\bar{1}0)$); as seen in Table 5, the observed peak frequencies are different in the three groups of tourmalines. The Raman spectra contain four intense

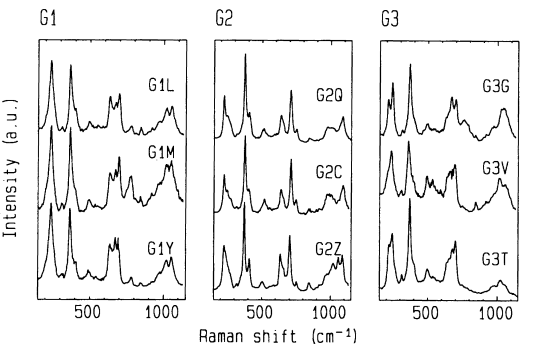

Fig. 2. Experimental Raman spectra of tourmalines in groups G1, G2 and G3 in $x(zz)\bar{x}$ and $x(zy)\bar{x}$ polarization geometry.

spectral bands centred at about 230, 370, 670 and 1020 cm^{-1}. The first band originates mainly from Mg-O and Fe-O bond stretching, while the second arises from Al-O bond stretching modes, the third from symmetrical Si-O-Si vibrations and the fourth from Si-O bond stretching. The most marked differences between the three groups of tourmaline are observed for the low-frequency band (LFB) at about 230 cm^{-1} and for the mid-frequency band (MFB) and about 670 cm^{-1}. The latter arises from Si_6O_{18} ring vibrational modes, localized in the bridging oxygen atoms, whose frequencies are strongly influenced by the Y-cations (Mihailova et al., 1996), while the band at 230 cm^{-1} is directly controlled by Y-O bond stretching. Therefore, using these two bands, one can estimate the type of predominant cations in Y-positions:

- tourmalines of buergerite-shorl type (G1), in which more than a half of the *Y*-positions are occupied by Fe. Their spectra are characterized by a single peak at 238 ± 2 cm^{-1} in the LFB and three resolved peaks at 635 ± 3, 674 ± 3 and 697 ± 3 cm^{-1} in the MFB.
- tourmalines of elbaite type (G2), characterized by a sharp peak at 224 ± 2 in the LFB, and two well-separated peaks in the MFB with frequencies at $638 \pm 3 cm^{-1}$ (asymmetrical) and higher than 707 cm^{-1} (sharp symmetrical).
- tourmalines close to the dravite type (G3), in which more than a half of the *Y*-positions are occupied by Mg. Their spectra are characterized by two peaks in the LFB, at 215 ± 3 and 237 ± 3 cm^{-1}, while only one peak, at $698 \pm 4 cm^{-1}$, can be resolved in the MFB. The type of *Y*-positioned cations also influences the O-H bond stretching modes which generate peaks with frequencies above 3000 cm^{-1}, a problem that is to be considered in future research.

Thus, Raman spectroscopy, in addition to X-ray diffraction and other methods for studying the structure, can be successfully used for obtaining valuable information on the short- and intermediate-range ordering in tourmalines.

References

Alvarez, M.A. & Coy-Ill, R. (1978): Raman spectra of tourmaline. *Spectrochim. Acta,* **34A**, 899–908.

Buerger, M.J., Burnham, C.W., Peacor, D.R. (1962): Assessment of the several structures proposed for tourmaline. *Acta Cryst.,* **15**, 583–590.

Foit, F.F. Jr. (1989): Crystal chemistry of alkali-deficient schorl and tourmaline structural relationships. *Am. Mineral.,* **74**, 422–431.

Foit, F.F. Jr. & Rosenberg, P.E. (1977): Coupled substitutions in the tourmaline group. *Contrib. Mineral. Petrol.,* **62**, 109–127.

Griffith, W. (1969): Raman studies on rock-forming minerals. Part I. Orthosilicates and cyclosilicates. *J. Chem. Soc.,* (**A**), 1372–1377.

Hawthorne, F., Mac Donald, J., Burns, P. (1993): Reassignment of cation site occupancies in tourmaline: Al-Mg disorder in the crystal structure of dravite. *Am. Mineral.,* **78**, 265–270.

Mihailova, B., Gasharova, B., Konstantinov, L. (1996): Influence of non-tetrahedral cations in Si-O vibrations in complex silicates. *J. Raman Spectr.,* **27,** 829–833.

Mihailova, B., Zotov, N., Marinov, M., Nikolov, J., Konstantinov, L. (1994): Vibrational spectra of rings in silicate glasses. *J. Non-Cryst. Solids,* **167**, 265–274.

Peng, M., Mao, H.-K., Chen, L.G., Chan, E.E.T. (1989): The polarized Raman spectra of tourmaline. Ann. Rep. of the Director of the Geophysical Laboratory, Carnegie Inst. Washington, 1988–1989, Geophysical Laboratory, Washington, D.C., 99–105.

Received 5 January 1996
Modified version received 22 July 1996
Accepted 28 May 1997